JIMMA UNIVERSITY

SCHOOL OF GRADUATE STUDIES

DEPARTMENT OF CHEMISTRY

RESEARCH THESIS ON

Effect of Sulphur and Nitrogen Co-Doping On Energy Bandgap, Antioxidant and Antimicrobial Activity of Zinc Oxide Nanoparticles

APRIL, 2023

JIMMA, ETHIOPIA

Effect of Sulphur and Nitrogen Co-Doping On Energy Bandgap, Antioxidant and Antimicrobial Activity of Zinc Oxide Nanoparticles

RESEARCH PAPER SUBMITTED TO SCHOOL OF GRADUATE STUDIES JIMMA UNIVERSITY IN PARTIAL FULFILLMENT OF THE REQUIREMENTS FOR THE DEGREE OF MASTER OF SCIENCE IN PHYSICAL CHEMISTRY

By
Diriba Yadesa

Advisors: **Tamene Tadesse (PhD)**

Jabessa Nagassa (MSc)

SCHOOL OF GRADUATE STUDIES

JIMMA UNIVERSITY

COLLEGE OF NATURAL SCIENCES

We, the undersigned, members of the Board of Examiners of the final open defense by _____have read and evaluated his thesis entitled**'' ---Title---''** examined the candidate. This is therefore to certify that the thesis has been accepted in partial fulfilment of the requirements for the degree Master of Science **in Chemistry (Physical)**.

_____	_____	_____
Name of the Chairperson	Signature	Date
_____	_____	_____
Name of Major Advisor	Signature	Date
_____	_____	_____
Name of Co-Advisor	Signature	Date
_____	_____	_____
Name of Co-Advisor	Signature	Date
_____	_____	_____
Name of the Internal Examiner	Signature	Date
_____	_____	_____
Name of the External Examiner	Signature	Date

Table of Contents

List of figures

List of tables

List of appendices

LIST OF ACRONYMS

ACS	Ascorbic acid
DDPH	diphenyl picrylhydrazyl
FTIR	Fourier transformed infrared
MO	Metal oxide
NF	Nano flower
NPs	Nanoparticles
NW	Nanowires
TE	Tissue engineering
UV-VIS	ultra violet visible
XRD	X-ray diffractometer
ZnO	Zinc oxide

Abstract

Semiconducting MO-NPs have been taken into consideration for their important applications like fast and profound detection, portability, high antimicrobial action, and relatively low cost compared to other conventional procedures. . Zinc oxide nanoparticles can safely be used as medicine, preservative in packaging, and photo catalysis and antimicrobial agents. It easily diffuses into the food material, kills the microbes, and prevents a human being from falling ill.

The XRD result imiply some additional peak patterns with S-N-co-doped was observed which resulted from residual or incomplete converson of complexe compound S and N of synthesized nanoparticles even though a hexagonal structures of ZnO is not changed. In addition there was slightly change in diffraction angle both towards the lower and higher angle in 6%N-ZnO, as a result of ionic radius and bond length difference respectively as it was reported in other literatures. Crysal size of synthesized NPs has been calculated using FWHM , and the size of N-S-dual doped ZnO NPs has smallest compare to the single doped and pure ZnO NPs .The UV absorption spectra showed redshifts from 370 toward 377 nm and 378 nm due to the nitrogen and sulfur doping respectively while 370 towards 379 nm due to S-N-co doping. Accordingly, the approximated energy bandgap values for bare ZnO-NPs, 6%N-ZnO, 4%S-ZnO and S4-N6-ZnO were 2.97, 2.78, 2.69 and 2.63 eV respectively. From this, the S4-N6- ZnO NPs has minimum energy bandgap. The study results revealed that ZnO NPs functionality is modified by dual doping of S and nitrogen.doped and co-doped nanoparticles had good crystalline nature, and structures of hexagonal wurtzite. All undoped ZnO, 6%N doped, 4%S doped and S4-N6- co-doped ZnO nanoparticles demonstrated worthy antibacterial and antifungal activity against four bacterial strains and one fungal genus. Generally, S-N-co doped ZnO NPs were found to be possess more antimicrobial activities than undoped ZnO NPs.

Keywords: ZnO-NPs, Antimicrobial, Enegy bandgap, Characterization, co-doping, Anti-oxidant

Acknowledgement

I would like to acknowledge Almighty God for his grace, un limited mercies, strength, and good health as I undertook this research. My sincere gratitude to my advisor give Dr Tamene Tadesse and Mr Jabessa Nagasa for their friendly approach, readiness and willingness to advice on this research, commitment to guide and support greatly improved this thesis work.

Besides to my advisor, I would like to thank to my wife Mrs Sufe beyene for her constant moral support and took responsibility in family guidance.

Last but not least I would like to thank all my classmates, friends for their moral support and love.

1. Introduction

1.1 Background of the study

Nanotechnology is an interdisciplinary subdivision of science, which stresses the study of materials in the Nano-range (1-100 nm). The tremendous evolution in the field of nanotechnology has revealed new essential and applied frontiers in material science and engineering [1-3]. Among the various categories of nanomaterials, metal oxide nanoparticles (MONPs) are pretty for a large variety of applications including catalysis, optoelectronic materials, sensors, and environmental remediation. The metal oxide nano materials have been potentially used in biomedical applications, which may be due to the high surface area of metal oxide NPs. It has considerably enhanced its ability to produce reactive oxygen species (ROS) .ROS production may be effected by various paths such as irradiance of nano materials by ultraviolet (UV) light, disturbance of intracellular metabolic activities, and antioxidant system. This results in the generation of oxidative stress in the cells. ROS can cause cell death in DNA, cell membrane and proteins,

Some of the most common MONPs include Ag_2O, CuO, ZnO, TiO_2, Al_2O3, CrO_2, NiO and others [4]. Among these MONPs, Zinc oxide nanoparticles (ZnO-NPs) have drawn great attention from researchers for therapeutic and diagnostic purposes, due to their reduced toxicity, biodegradable nature and low cost [3]. Zinc oxide nanoparticles can safely be used as medicine, preservative in packaging, photo catalysis and antimicrobial agents. It easily diffuses into the food material, kills the microbes, and prevents a human being from falling ill [5]. Moreover, it highly increases the photocatalytic degradations of some persistent dyes that induce severe environmental pollution.

However, its wide band gap of ZnO (~3.37 eV) [6-7], a large exaction binding energy of 60 meV [8, 9], and agglomeration [10, 11] hinder it from potential applications [3, 5]. functionality and efficiency of ZnO NPs can be improved by increasing and modifying their surface area by adding some dopants materials i.e. biomolecules and transition metals (Mn, Fe, Cr, Cu) at nano scale this techniques to enhance a major portion of sunlight and enhance the optical properties[7]. For improve such problems doping represents a good mechanism to modify ZnO NPs properties. Doping consists of the insertion of a specific ion into a crystal lattice, not originally present in the starting material. It can be particularly useful to minimize the energy band-gap with a direct consequence on the ZnO antioxidant properties and related antimicrobial activity. [10] The doping ZnO with other material did not change the precursor's material rather than create new functionality. In addition of doping, the physical and chemical behaviours of ZnO-NPs could be tuned by changing the morphology using different synthesis routes and materials [5]. Preparation of ZnO-nanocomposites improves the drawbacks associated with the bare ZnO-NPs. Nanocomposite materials can exhibit individual properties such as mechanical [12], chemical, electrical, optical and catalytic properties [2, 3] which make them preferable compared with their respective individual nanoparticles. It is also considered as safe material from the Food and Drug Administration, which makes it suitable for a plethora of biomedical applications in drug delivery systems [3]. Various ZnO NPs have been successfully applied in tissue engineering (TE) [4], nano flower NF [5] and nano wires (NW) [6]. Which have been found to promote the adhesion, growth, and differentiation of several cell lines Researchers indicated that the incorporation sulfur into ZnO-NPs while varying temperature has reduced band gap energy of ZnO –NPs, from 3.34 to 3.22 eV by other authors [9]. Moreover, the Ag-N-co doped of ZnO-NPs was also investigated by different authors along with its effect on energy band gap and photo catalytic degradation of organic pollutants [11]. Even though S-doped and Ag-N-co doped of ZnO-NPs have been already done and reported by others, the effect of S-N-co doping on energy band and its antimicrobial activity is still not investigated by others. The present study focus on minimize the energy bandgap, enhancing application towards antimicrobial and antioxidant activity of ZnO-NPs by S- N co doping.

1.2 Statements of the problems

MO-NPs have been taken into consideration for their important application like fast and profound detection, portability, high microbial action, and relatively low cost compared to other conventional procedures. However, their potential applications are restricted due to their high-energy bandgap and high electron–hole recombination in visible region of the electromagnetic spectrum as it has been reported in different literatures [12]. To improve such problems, doping of trace amounts of metals and non-metal represents a good mechanism to modify ZnO-NPs properties. Researchers have reported single metal and non-metal doping on the Physico-chemical properties of ZnO-NPs and obtained good result. In this work, we have investigated the effect of dual non-metal doping on Physio-chemical of ZnO-NPs related to further reduction of its energy band gap and boost its antimicrobial and antioxidant behavior. Accordingly, we have investigated the effect of S & N co-doping of ZnO-NPs on its antimicrobial and antioxidant activity. Worthy band gap reduction of ZnO-NPs was obtained from the synergistic effect of the two non-metal having distinct properties compared to the single doped one. Following the appreciable energy band gap reduction, the antimicrobial and antioxidant behaviors of the pure ZnO-NPs was boosted largely. The research questions that had been answered in this study involve:

1. Why doping a single element was not so successful in narrowing bandgap energy in ZnO-NPs?
2. Did S-N-co doping narrow the band gap energy of ZnO-NPs?
3. Did S-N-Co doping capable of killing microbes?
4. Did S-N-Co doping active towards antioxidant?

1.3 **Objectives of the Study**

1.3.1 General objective

This study aimed to evaluate the effect of S-N-co doping on the energy band gap and the antimicrobial activity of ZnO-NPs.

1.3.2 Specific objective

The specific objectives of this study were

- ✓ Prepare S-N-co doped using ZnO-NPs as a control.
- ✓ To minimize the energy bandgap of ZnO-NPs by using S-N-Co doping.

- ✓ Examine the antimicrobial activity of S-N-Co doped ZnO NPs.
- ✓ Evaluate the antioxidant activity of undoped, doped and co-doped nanoparticles.

.

2. Review of Related Literature

2.1 The theoretical concept of ZnO-NPS

ZnO-NPs based drug delivery systems have been got high consideration in recent times [1]. In addition to the standard, the inclusion of nanoparticles with a high surface area as drug carriers has highly improved the encapsulation efficiency of drugs like pharmacokinetics and bio distribution of the drug [13.] Moreover, nanoparticles have been also investigated as antibiotics due to their promising antimicrobial activity and regulating bacterial infections often present after surgery to remove/replace organs and tissues [14]. Successful application of nano particles for treatment of cancer cells was due to its important physical and chemical properties like high surface area to volume ratio, the rich surface chemistry, the reduced size (1–100 nm), and spontaneous biodegradation which proof accumulation within the body once therapeutic action has been completed [15]. ZnO-NPs can also apply as tissue engineering (TE) to promote the repair damaged tissues and organs. Nanoparticles can show biocompatible characterizes in some cases, since its size matched with the nanometric scale of components present in the extracellular matrix of tissues [16].

2.2 Materials for doping ZnO-Nanoparticles (NPs).

ZnO is an inorganic material that has been successfully applied in different fields, starting from gas sensing [17] and energy harvesting to biomedicine [18]. For more application, it may be useful to optimize the functionalities to ZnO by adding other material (ions) rather than to improve the pre-existing ones, with the

final aim to design a multifunctional system. This can be approved by insertion of selected elements in the ZnO NPs which can be specifically useful to modulate the energy band-gap, with a direct consequence on the ZnO photo catalytic properties and related antimicrobial activities. ZnO offers a high driving force for reduction and oxidation processes because of its unique chemical and physical properties [19]. In addition to the generation of a weak ferromagnetic behavior in the doped particles [20], it causes the tuning of degradation properties in aqueous environments [21]. Or the modulation of the electromechanical response [22] Were the most important functionality modification resulted from the insertion of selected elements in the ZnO- nano particles (NPs). Fe [23], Mg [24], Ta [25] and Cu [26] are doped ZnO NPs with enhanced antimicrobial activities has it been reported. Generation of Reactive Oxygen Species (ROS), metal ion release and membrane damage [27] is the inhibitory mechanism of ZnO -NPs which enhance the antimicrobial activities of metal doped ZnO. This mechanistically improvement comes due to the enhanced generation of reactive oxygen species (ROS) as a result of doping [28]. Rare earth (RE), or lanthanide, elements are widely applied for the doping ZnO nanoparticles and to properly modify the corresponding electronic band structure [29]. In case of UV light irradiation, ZnO represent a very fast recombination of the photo generated charge carriers. Due to the 4f configuration use of lanthanide may help in increasing the recombination time of the electron/hole pair in the semiconductor [30], improving the efficiency of photo catalytic process, along with its antimicrobial activities.The change in the band-gap and the generation of trap states make RE doping interesting; the possibility of doped ZnO being used as an imaging agent also indicated from the luminescence point-of-view. The trap states induced by doping may act as radiative recombination sites not present in the pure crystal and the dopant atoms with aspects such as the crystallite size, contribute to change the band-gap of the system, resulting in the possibility to tune the optical properties of ZnO [31]. Increasing the absorption of light and lowering the recombination of photo generated charge carriers by incorporation of non-metals like (S, N,C) can affect the crystallization and structural properties of ZnO which can modify the photo catalytic activity Similarly, the N-doped ZnO also helps in the band-gap narrowing as well as the band-gap shifting towards the visible-light region. The non-metal doping in ZnO is very beneficial for improving its properties in optoelectronic applications as well as in the environmental purification [32].

2.3 Sulphur doped ZnO NPs

Incorporation of chalcogens into ZnO NPs was not familiar in the beginning times. However, recently, due to the large electro-negativity and size difference between S and O, S doping is one of the best ways to modify structural and optical properties of ZnO which, widely used for the remediation of environmental pollution [33]. the substitution of S in place of O affects the lattice constant which is responsible for the variation in electrical and optical properties of the semiconductor as result of the larger size of S^{2-} than that of O^{2-} [34].Different types of synthesis techniques like hydrothermal method [35]. Chemical bath deposition method [36]. Electrochemical deposition [37], one-step catalyst free thermal evaporation process [38].Mechano chemical approach, and wet-chemical approach were used for the preparation of different types of ZnO/S [39].In terms of simplicity, convenient, low cost, low growth temperature and eco-friendly, the hydrothermal process was the best method for the preparation of ZnO and ZnO/S [40]. In addition, great crystal quality, less intrinsic defects, different distribution of intrinsic defects and good electrical properties was obtained by using this method. [35]. In the hydrothermally synthesized Ag/S co-doped ZnO, it was found that Ag acts as a good successor and overcomes the generation of interstitial Zn and O vacancies while S enhances the solubility of Ag in the co-doped samples [37].

2.4 Nitrogen doped ZnO-NPs (nanoparticles)

Currently, nitrogen-doped ZnO NPs are a unique and attractive issue [41].Nitrogen is considered as the most effective dopant for p-type ZnO due to its atomic size being similar to that of oxygen. In addition, group V elements such as phosphorus (P) [42], arsenic (As) [43], antimony (Sb) [44], Are the most reliable dopants for p-type ZnO. Research on doping N and N_2 in ZnO has revealed that N_2 at the Zn site acts as a shallow recipient, and at the O-site, it acts as a donor, while N acts as a deep recipient as it reported by others [45]. N-doping in ZnO causes narrowing of the band gap in ZnO and increases the absorption of visible light [33].A number of methods such as molecular beam epitaxy, active sputtering, chemical fumes, and ZnO ammonolysis at low temperatures are used for producing nitrogen-doped ZnO. Using the proper nitrogen supply and introduction of it into ZnO-NPs using a solution combustion method is a simple, but promising method of nitrogen fixation in oxide. The photo catalytic activity of ZnO towards the breakdown of organic dyes is increased by enhanced VL absorption, which is assigned to the formation of localized states of N 2p in the band gap. The behavior of nitrogen dopants in ZnO has been

discussed by theoretical calculations, such as the ab initio electronic band structure method [46] and density functional theory [47].

2.5 Antimicrobial activity

The issues related to resistant of microorganisms facilitate the study of new and more effective antimicrobial agents. Good antimicrobial effects have been obtained from metal oxide nanoparticles, such as MgO, Cu_2O, CuO, ZnO, TiO_2, and WO_3, which present distinct behavior and properties from micrometric or millimetric particles. ZnO-NPs found as an antimicrobial agent against both pathogenic and spoilage microorganisms as it has been reported earlier.

In some cases ZnO NPs proven as potential antimicrobial agents for Staphylococcus aureus and Escherichia coli which is mainly found in urban waste water. [48]

Their proposed mechanisms for antimicrobial activity may be due to induction of oxidative stress which resulted formation of reactive oxygen species, membrane disruption due to the accumulation of ZnO-NPs therein, and internalization of nanoparticles followed by the release of antimicrobial ions (Zn^{+2}). In addition to its unique antibacterial properties, ZnO is classified as a Generally Recognized as Safe (GRAS) compound by the U.S. Food and Drug Administration (FDA, 2016). [50].

Surface area and concentration are more pronounced than crystalline structure and particle shape for the antimicrobial activity of ZnO nanoparticles. The smaller size of ZnO particles better is its antimicrobial activity. Thus higher the concentration and larger the surface area of the nanoparticles, the better is its antimicrobial activity. Some researchers have proposed in their study that the generation of hydrogen peroxide is the main factor of the antibacterial activity, while it also indicated that the binding of the particles on the bacterial surface due to the electrostatic forces could be another factor [51].

The issues of controlling the growth of pathogenic microorganisms are one of foremost importance for food safety and public health. Different bacteria are causes major opportunistic human infections in different ways. They are common soil and water bacteria which widely distributed among fresh foods. Bacillus_cereus is a pathogenic bacterium commonly isolated from soil and easily spread in the environment. Humans are the primary reservoir of S. aureus, and food

contaminated during its preparation is the most significant source of staphylococcal food poisoning. Salmonella spp. is a resilient bacterium capable of adapting to temperature, pH, and water activity beyond their normal growth range, posing high risks to safety.

The present study aimed to study the effect of sulphur and nitrogen co-doping on the energy bandgap and evaluate their antimicrobial and antioxidant activity of ZnO-NPs.

2.6. Antioxidant activity

Treatment of Cancer by chemotherapy, radiation therapy and surgery were efficient towards the killing of cancer cells, however it has been diminished in current times since it has an adverse effect towards the normal cells also.1–3 this improved as result nano medicine generation. ZnO NPs have advanced imaging, therapeutic activity and effective for early detection of cancer and its treatment.

ZnO NPS exhibit the antioxidant activity regarding mechanisms free radical scavenging and reducing activities. Additionally, ZnO-NPs are protected cell membranes against oxidative damage, decrease free radicals and malondialdehyde (MDA) levels, and increase the antioxidant enzyme levels. Rattt. Antioxidants play an important role in the functioning of all bio systems.

3. Materials and methods

To determine the impact of S-N-Co doping on the bandgap energy of ZnO-NPs were prepared by the sol-gel technique and mixed with different ratios of ZnS and $(NH_2)_2CO$ respectively [9].

3.1 Chemicals and instruments

Chemicals like hexahydrated zinc nitrate (Zn $(NO_3)_2).6H_2O$), sodium hydroxide (NaOH), ethanol (C_2H_5OH), zinc sulphide (ZnS), urea $(NH_2)_2CO$, 2, 2-diphenyl-1- picrylhydrazyl (DPPH) and ascorbic acid were purchased and distilled water were used in this research work. ZnS and $(NH_2)_2CO$ were used as sulphur and nitrogen sources for doping, respectively.

Different apparatus and materials, such as beakers, measuring cylinders, magnetic stirrers, an electronic beam balance, a muffle furnace, burettes, funnels, filter paper, a pH meter, sample bottles, centrifuge tubes, sample vials, and aluminum foil, were used.

Advanced analytical instruments such as x-ray diffractometry (XRD), an UV-vis spectrometer, and a Fourier transform infrared (FTIR) spectrophotometer were used for this research.

3.2 Preparation of ZnO-Nps: ZnO-Nps were synthesised by sol-gel techniques. For the preparation of ZnO—NPs, 6 g of hexahydrate zinc nitrate was dissolved in 50 mL of distilled water at room temperature. Next, 0.8 g of sodium hydroxide was mixed with 100 mL of temperate distilled water at room temperature. Constant stirring was done for both solutions for 30 minutes with a magnetic stirrer[52].

Following that, NaOH solution was poured into the solution drop wise while constant stirring was maintained, adjusting the pH until it reached 10. After the pH was adjusted, the mixed solution was heated on a hot plate at 60 °C for 2 hours while vigorous stirring was done continuously. The solution left for cooled and filtered by what man filter paper and washed three times with distilled water and ethanol respectively. The filtered samples were dried in an oven at 60 °C and calcined at 500 °C on muffle furnace for 2 hours. Finally, the white powders were obtained, which confirmed the colour of ZnO-Nps [53].

3.2.1 Preparation of N-ZnO-Nps: Different concentrations of urea were prepared by dissolving 0.015, 0.03, 0.045, and 0.06 g in 25 mL of distilled water at room temperature. Each concentration of urea was added to the previously prepared solution of hexahydrated zinc nitrate and stirred for 10 minutes to obtain a homogenous solution. Sodium hydroxide solution (2 M) was prepared separately by dissolving 0.8 g of NaOH into 100 mL of distilled water. The sodium hydroxide solution were added drop wise to the solution that contain zinc nitrate and urea solution until it forms precipitate while controlling pH. Then the mixed solution heated at 60 ^{0}C while constant stirring for 2hr. the solution kept to cooled and filtered by what man filter paper and dried on oven at 60 ^{0}C and calcined on muffle furnace at 500 ^{0}C for 2 hr.[54]

3.2.2 Preparation of S-ZnO-Nps: ZnS solution was made by dissolving various amounts (0.01, 0.02, 0.03 and 0.04 g) into 10 mL of distilled water. The produced ZnO-Nps (1g) was then dissolved in 10 mL of ethanol, combined with the ZnS solution, and stirred for 3 hours at room temperature. Finally, the mixed S/ZnO solution was filtered, rinsed with distilled water till the pH of the removed waters reached 7, air-directed overnight, and calcined at 300 ^{0}C for one hour [52].

3.2.3 Preparation of S-N- co –doped ZnO-Nps: S-N-Co doped was prepared from the zinc oxide nanoparticles by dissolving 1g of ZnO into 10 mL of ethanol and mixed with selected amount urea solution and zinc sulfide solution separately. Following that stirred at room temperature for three hours, filtered and rinsed with distilled water until pH of removed water reaches 7, Air directed overnight, and calcined at 300 °C for one hour.

3.2.4 Characterization of synthesized Nano particles (NPs): The synthesized nanoparticles of bare, doped and co-doped ZnO nanoparticles were characterized by X-ray diffraction (XRD),

UV−vis, and FTIR spectroscopic techniques. A 0.2 M concentration of each sample was prepared in ethanol for UV−vis, but XRD and FT-IR were used for measurements of solid powders. The diffraction measurements were conducted on a Drawell XRD-.using Cu Kα radiation over a 2θ in the range of 10−80°. Absorbance measurements were conducted with UV−visible spectrophotometer for the determination of bandgap energies.

3.2.5 Antimicrobial activity test

Antimicrobial studies were conducted at the Jimma University in the Biology Department Laboratory and done using the agar disc diffusion method [1]. The biological screening effects of the synthesized nanoparticles were tested against the bacterial strains such as,Staphylococcus *aureus*, sallamonela typhis, Bacillus cereus and Escherichia coli and fungal activity was also tested against *Candida alibican.* Culture containing test tubes with approximately equal concentration or density of 0.5 McFarland standard was used for inoculation of media[55]. And freshly grown liquid culture of test bacteria and fungi solution having similar turbidity with 0.5 Mc Farland were seeded over Muller-Hinton Agar (MHA) and Potato Dextrose agar respectively. DMSO was used as negative controls while Gentamycin and clo used as positive control for bacteria and fungi respectively. The sample solution of 100 mg/ml of each tested compound has been prepared by dissolving the compounds in DMSO and the solutions were loaded on the wells of the culture and in culture incubated at 37 °C for 24 hours. The inhibition zones were developed on the plate around the standard paper disc with adiameter of 6 mm, and the antimicrobial activity of nanoparticles was demonstrated by the diameter of the zone of inhibition developed around the sample.

3.2.6 Antioxidant activity test

A DPPH radical scavenging assay was performed to determine the ability of the prepared ZnO NPs to scavenge free radicals. The ability of NPs to inhibit oxidation was tested by decolourizing a methanol solution of DPPH. In methanol solution, DPPH creates a violet/purple colour, which fades to shades of yellow in the presence of antioxidants. A 0.1 mM DPPH in methanol solution was prepared and 1ml of it was combined with 3 mL of bare ZnO-NPS, 6%N-ZnO, 4%S-ZnO and S4-N6-ZnO in methanol at (70, 90,110,130 Mg/mL) for each nanoparticles. The reaction mixture was vortexed completely and kept at room temperature for 30 min in the dark [8]. At 517 nm, the

absorbance of the mixture was determined spectro photometrically. Ascorbic acid was used as a standard. The following equation was used to compute the percentage of DPPH radical scavenging activity:

$$\% \text{ DPPH radical scavenging activity} = \frac{(A_O - A_1)}{A_0} X\ 100$$

Where the absorbance of the control is A0 and the absorbance of the sample is A1. The percent of inhibition was then plotted against concentration, and the IC50 was derived from the graph. At each concentration, the experiment was performed three times.[56]

4 .Result and discussion

4.1 production of zinc oxide nanoparticles.

By sol –gel techniques, ZnO NPs was obtained successfully. Hydrolysis of Zn $(NO3)2.6H_2O$ with NaOH results formation of ZnO colloid. Causing to heating, Zn $(NO3)2.6H_2O$ within solution leads to productions of nitrate ions and zinc ions. Zinoc hydroxide nitrate is an intermidate product of the hydrolysis reaction formed in the presence of H_2O and OH^-.The formed intermidate is directly converted into ZnO upon heating and through long time refluxing.$NaNO_3$ is water soluble and easily separated from the obtained products. During drying, Zn $(OH)_2$ is totally converted to ZnO by the follow reaction:

$$Zn(NO_3)_2.6H_2O\ (aq) + 2NaOH\ (aq) \longrightarrow Zn(OH)_2\ (s) + 2NaNO_3\ (aq) + 6H_2O\ (l)$$

formation

$$+ \quad Zn(OH)_2\ (s) \xrightarrow{\text{heating}} ZnO\ (s) + H_2O\ (g)$$

4.2 Characterization of synthesized nanoparticles

4.2.1 UV–Vis spectroscopy studies

The UV–Vis spectroscopy studies were performed to study the absorption properties of pure ZnO NPs 6%N-ZnO, 4%S-ZnO and S4-N6-ZnO. The energy differences between the highest occupied molecular orbital (HOMO) and lowest unoccupied molecular orbital (LUMO) formed by the hybridization of Zn d orbitals and oxygen 2p orbitals causes the bandgap, which in turn leads to absorption in the UV–Vis region. Fig. 1 shows absorption spectra of all prepared pure, doped and dual doped ZnO NPs .The absorption values are observed at 370 nm for ZnO and 376 nm, 377 nm and 379 nm for 6%N-ZnO, 4% S-ZnO and S4-N6-ZnO respectively. No additional peak is observed except redshift from ZnO to doped and dual doped ZnO NPs which indicates that the process of doping did not alter the crystal structure of ZnO NPs.

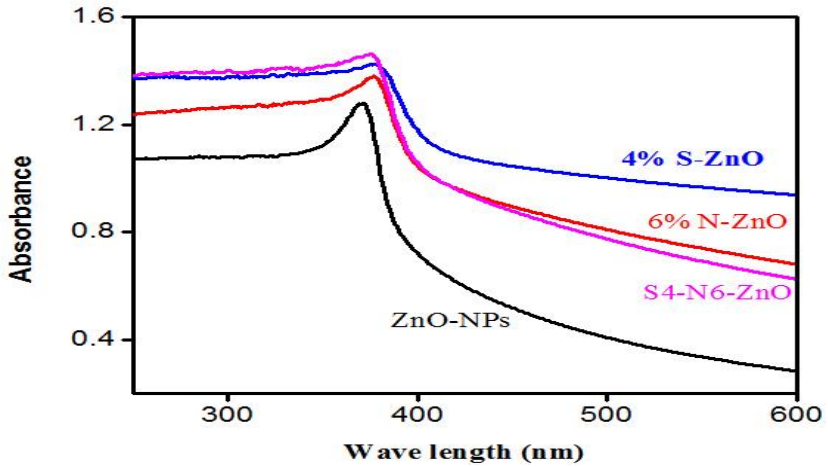

Figure 1. Ultraviolet-visible absorbance spectra of bare, doped and co doped quantities of nitrogen and sulphur zincoxides.

4.2.2 Optical Bandgap energy Analysis

The optical bandgap (Eg) was calculated using the Tauc method. A Tauc plot can be drawn using the UV–Vis absorption results and the following equation,

$$(ahv)^2 = \quad (hv - E_g)$$

Where a represents the absorption coefficient, h represents Planck's constant, v is the frequency of light and E_g is the optical band gap. Fig. 2 shows the Tauc graph, which is plotted between $(ahv)^2$ and hv using the above-mentioned equation, and where extrapolation of the linear part of the graph gives the band gap value. The calculated band gap values are 2.97 eV, 2.78 eV, 2.69eV and 2.63 eV for pure ZnO NPs, 6%N-ZnO, 4%S-ZnO and S4-N6-ZnO respectively. As expected, there is a difference in the energy band gap observed for doped and co-doped compare to pure ZnO NPs. Particularly, the energy band gap of S4-N6-ZnO has decreased when compared with that of pure ZnO NPs , 6%N-ZnO, and 4%S-ZnO. This may due to modification of electronic level of zinc oxide. More 2p electron of nitrogen compared to the substituted oxygen by N induce the new energy level between the conduction and valence band of ZnO, which results decreasing the band gap in ZnO NPs.(agn).

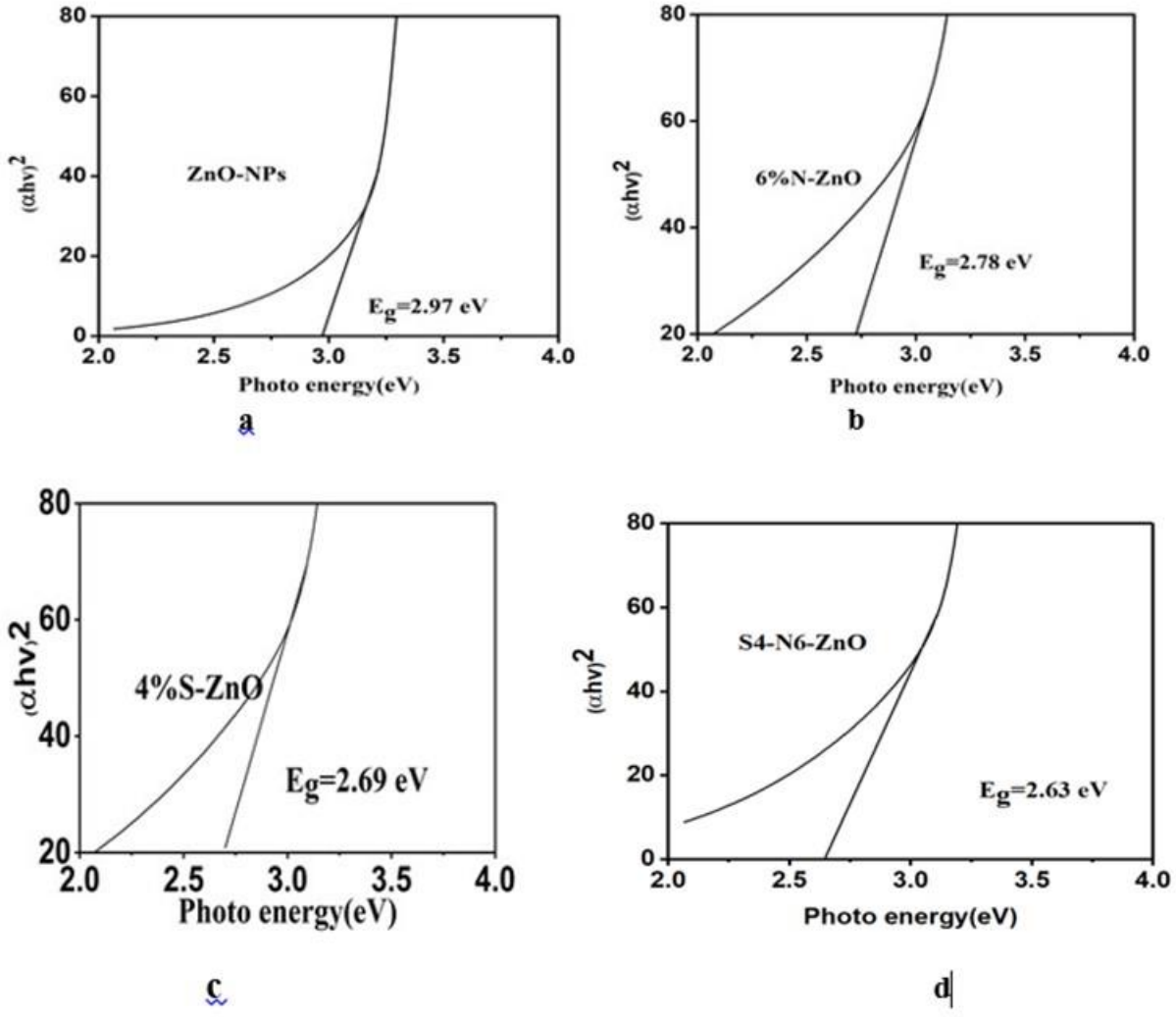

Figure 2. Energy Bandgaps of bare doped co-doped quantities of nitrogen and Sulphur. (a) Pure ZnO-NPs (b) 6%N-ZnO (c) 4%S-ZnO and (d) S4-N6-ZnO

4.2.3 FTIR –Analysis

Light transmittance properties were measured for bare, doped and co-doped ZnO-NPs by FTIR (Perkin Elmer Spectrum two) in the wave number range of 4000−400 cm−1. Figure 4 shows the IR spectra of ZnO-NPs, 6%N-ZnO, 4%S-ZnO and S4-N6-ZnO samples in order to see their difference in functional groups. The IR spectra prove that the zinc oxide absorption band with a stretching mode of Zn−O is between 400 and 850 cm^{-1}, which corresponds to the hexagonal ZnO crystal structure. The peaks observed between 3300 cm^{-1} and 3500 cm^{-1} are assigned to the O− H stretching mode of the hydroxyl group which comes from surface adsorption of water. These observations from the FTIR bands indicated the existence of impurities mainly near ZnO surfaces. In addition, there is a strong absorption peak observed at 877 cm^{-1} in all samples which assigned to replacement of the O by H .A new peak, which is not sharp, was observed at 1410 cm^{-1} due to microstructure formation of the sample (Zn−S) during doping and the peak at 1387 cm^{-1} corresponds to a Zn-N Stretching vibration and the peak around 2426 cm^{-1} is C=O streching.

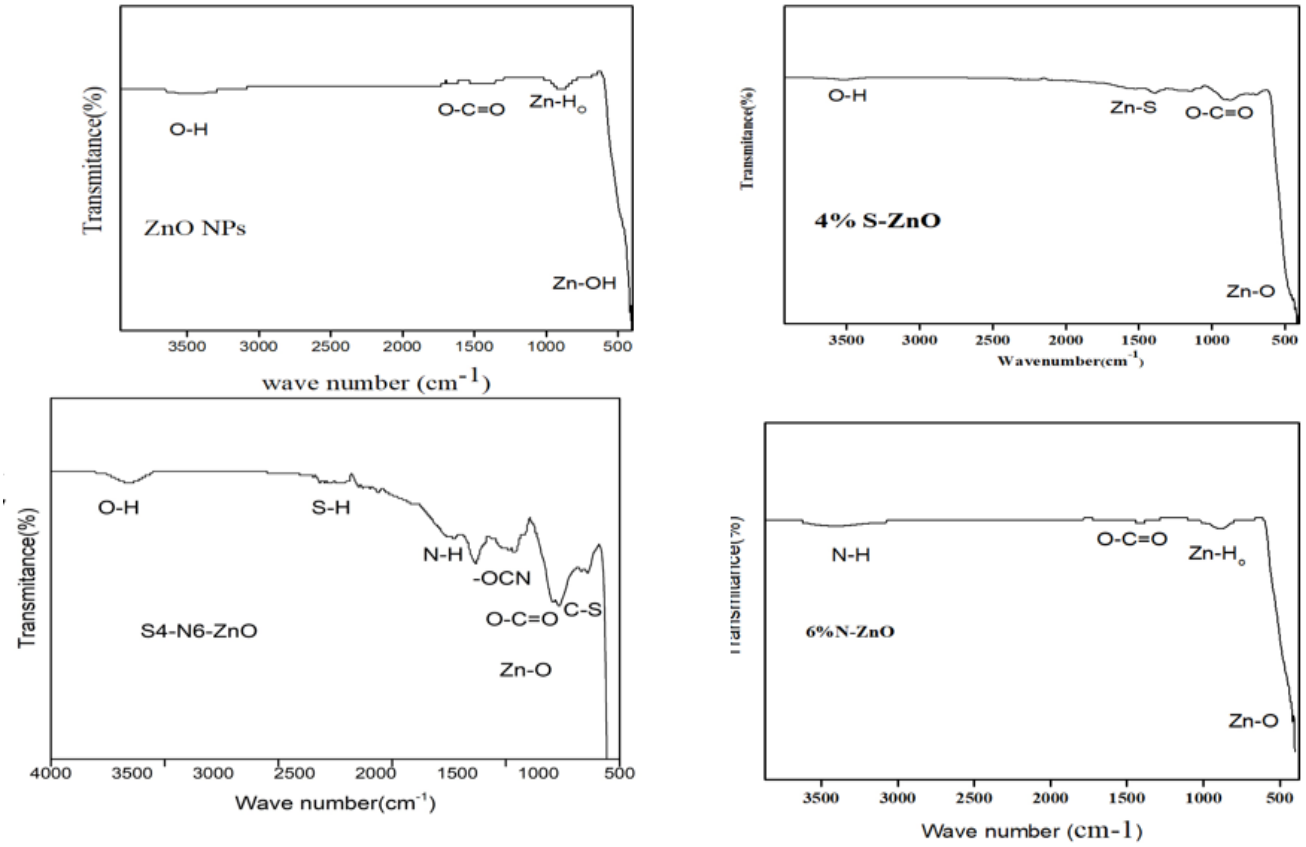

Figure 3. FTIR bands of bare, doped quantiaties of 6%N-ZnO, 4%S-ZnO and S4-N6-ZnO.

4.4.4 Powder X-ray diffraction (XRD) analysis

ZnO nanoparticles were synthesized from precursor Zn- $(NO_3)_2.6H_2O$ by the conventional sol−gel process. The obtained products were calcined at temperatures of 500, °C for 5 h, and then, the products were characterized employing Cu Kα radiation over a 2θ in the range of 10−80°. The XRD patterns of the produced products are revealed in Figure 4, which indicates the crystalline arrangement under the hexagonal structure (JCPDS) with leading peaks at 2θ = 28.62°, 31.86°,

34.62°, 36.28°, 47.64°, 56.78°, 63.15°, and 68.18°. These lines were indexed correspondingly as matched to the hexagonal phase of ZnO. The particles have a high crystallinity at 36.28° for both single doped and dual doped which was evidenced by a sharp peak as well as highest intensity. The progression of larger crystals from those of smaller size leads to a reduction in the number of smaller particles, while larger particles continue to grow.

Figure 4 exhibits the XRD patterns of un doped S-doped and N -doped ZnO-NPs; the precise peaks were located at (2θ) = 2θ = 28.62°, 31.86°, 34.62°, 36.28°, 47.64°, 56.78°, 63.15°, and 68.18°. The diffraction peaks of the S-doped ZnO-NPs and N- doped are close agreement with the pure ZnONPs and almost similar. This implies that sulfur and nitrogen atoms have been doped in the ZnO crystal and the absence of additional peak indicates that the occurrence of sulfur and nitrogen residual compounds or complexes are excluded from S and N doped ZnO NPs while addition peaks in S-N- co-doping shows the presence residual or complexe compound of S and N. On other hand, the intensity of diffracted peaks change with the dopant concentration. A decrease in the intensity of doping is due to a change in electron density. Generally, the intensity of the diffraction peaks decreases greatly through the S and N- dual dopant than single dopant. Indicating a relative loss of crystallinity due to lattice alteration.

The crystallite sizes of both pure , S-doped , N- doped and S-N-co doped ZnO-NPs have been achieved from the full-width at half-maximum (FWHM) of the supreme strong peaks of the corresponding crystals using the Dybe-Scherrer equation, $D= \frac{0.9\,\lambda}{\beta cos\theta}$ where λ is X-ray wavelength, D is the average crystallite size, θ is Bragg's diffraction angle, and β is the FWHM in radians. The crystallite size calculated based on the XRD result (by using the Debye− Scherrer equation) was decreased with the decreasing peak intensity due to the doping concentration. The calculated crystallite size (D) of synthesized NPs for most intense peaks are recorded in table 1.
The order of crystallite size synthesized NPs was: S-ZnO > ZnO NPs > S-N-ZnO > N-ZnO NPs. The lower size of S-N-ZnO and N-ZnO NPs was due to doping of N as the the N doped exhibited the lowest crystal size. (Table 1). The most noticeable tendency versus particle size is that the surface-to volume ratio increases for smaller particles.

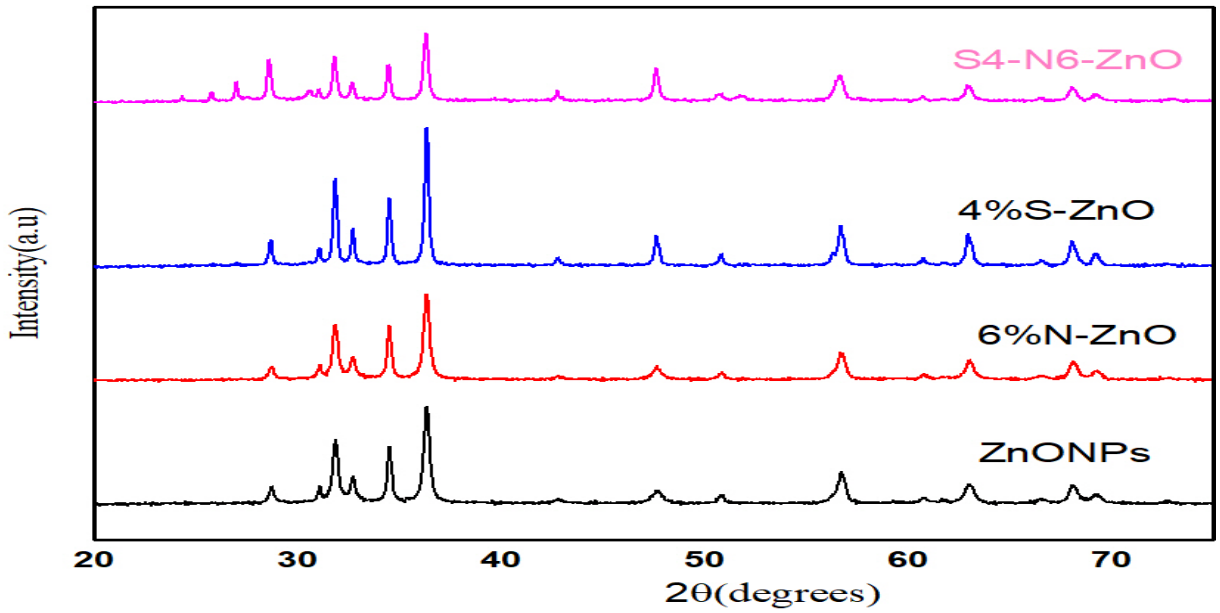

Figure 4. XRD pattern of pure ZnO-NPs, 6%N-ZnO, 4%S-ZnO and S4-N6-ZnO.

Table1: Calculated crystalline size of synthesized pure ZnO NPs, S-doped , N-doped and S-N-co doped ZnO NPs at 500 °C

4.5. SEM analysis

In order to elucidate the external structure of 6%N-ZnO, 4%S-ZnO and S4-N6, SEM analysis was performed. SEM images of pure ZnO-NPs, 6%N-ZnO, 4%S-ZnO and S4-N6 are shown in **Figure 5.** It can be easily observed the morphology of dual doped ZnO-NPs (S4-N6) is highly improved compared single doped and pristine ZnO-NPs. The crystal size of pure ZnO NPs ,6%N-ZnO 4%S-ZnO and S4-N6-ZnO are 29.06, 22.44, 29.21 and 25.76 nm respectively as it has been

calculated from XRD data. The morphology improvement is attributed to the modified stability and formation of surface charge as revealed by the FTIR analysis.

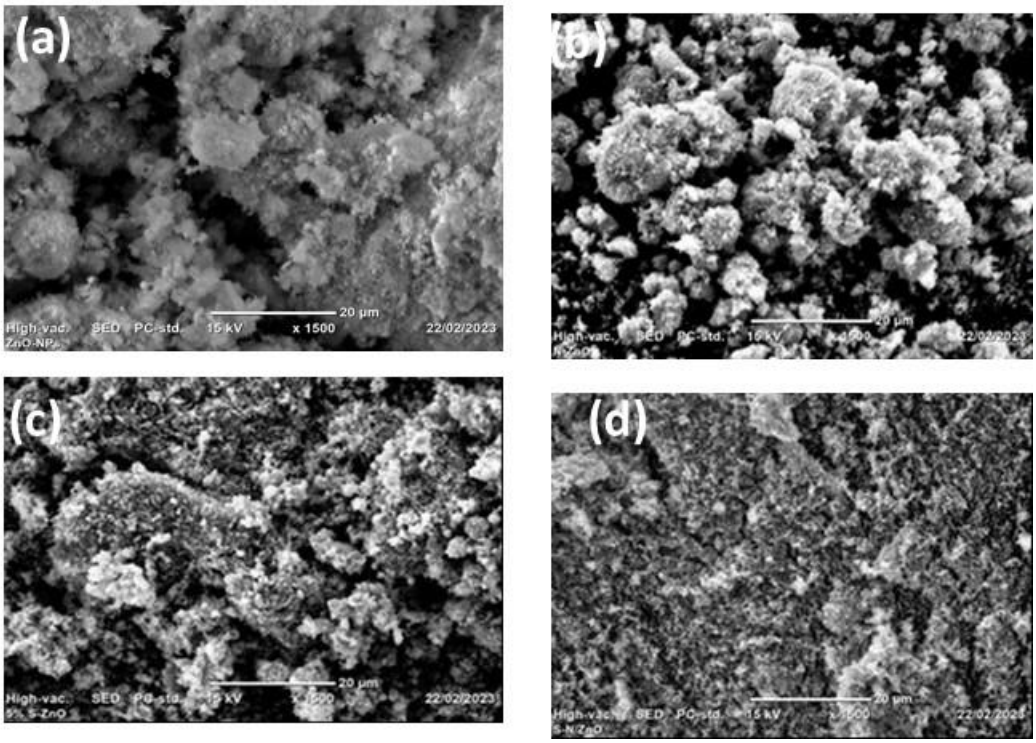

S/N	Synthesized nanoparticles	θ	cos θ	λ(nm)	β(radian)	D(nm)
1	ZnO NPs	18.18	0.78	0.154	0.0039	29.06
2	6%N-ZnO	18.18	0.78	0.154	0.0050	22.44
3	4%S-ZnO	18.18	0.78	0.154	0.0038	29.21
4	S4-N6-ZNo	18.18	0.78	0.154	0.0043	25.76

Figure 5. SEM image of (a) pure ZnO-NPs (b) 6%N-ZnO (c) 4% S-ZnO (d) S4-N6-ZnO

4.6 Antimicrobial activity analysis*

The antimicrobial activities of undoped ZnO, N doped ZnO, S doped and S-N-co doped ZnO NPs against Staphylococcus aureus, Salamonella typhi (-ve), Bacillus cereus, Escherichia coli (-ve) and Candida alibican were done using the disk diffusion method and the diagram for the zone of inhibition is indicated in **Figure 6**. The antimicrobial activity study results of undoped ZnO, 6% N doped ZnO and 4%S doped NPs were found to be effective against all bacteria strain and fungi. However, percentage reduction in bacterial growth was found to be significantly higher using S-N-ZnO NPs compared to that of the S- ZnO NPs and N-ZnO NPs. Thus, the antibacterial effective of synthesized NPs was more active for gram-positive bacteria as compared to gram-negative bacteria, which is similar with previous reports.. The possible reason behind this is different in (i) cell membrane structure, (ii) physiology and metabolic activities of the cell, and (iii) degree of contact of gram-positive and gram-negative bacteria. The antibacterial activity of single doped and dual doped ZnO nanoparticles showed that they were more resistant to gram-negative bacteria than gram-positive bacteria. Generally, 6%N doped ZnO NPs showed better antifungal activity when compared with undoped ZnO NPs, as it was indicated by inhibition zone in Table 1 and this is supported in earlier literature.[58]

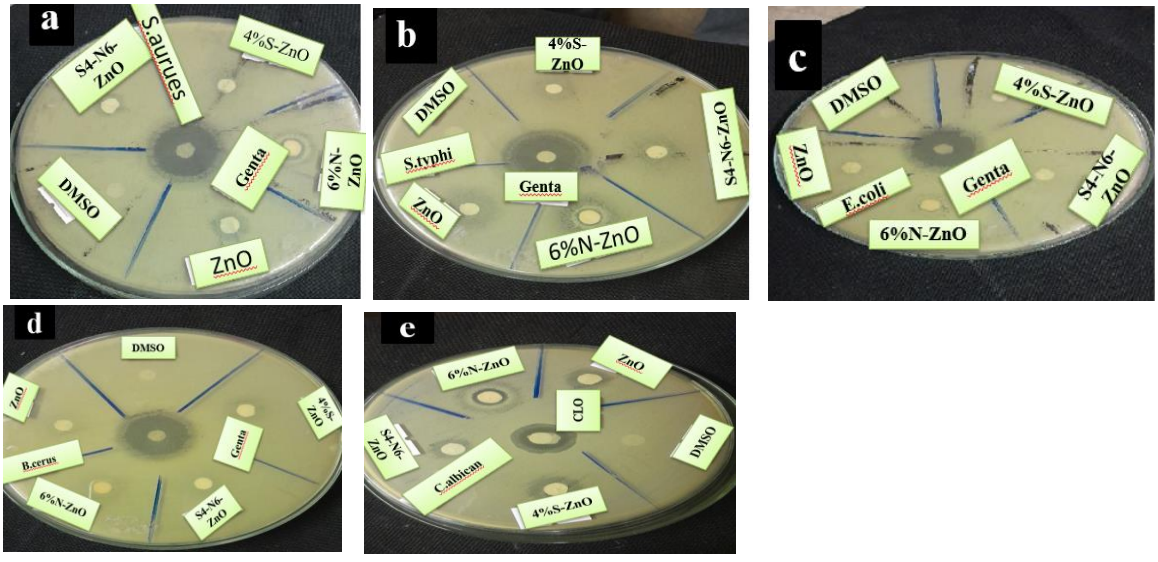

Figure 6. Diagrams showing of zone of inhibition the pure and doped ZnO-NPs against some selected microorganisms

Table2. Antibacterial and antifungal activity of ZnO, 6%N-ZnO, 4%S-ZnO and S4-N6-ZnO

Name of sample	Zone of inhibition (mm in diameter)				
	S.aureus	S.typhi	E.coli	B.cerus	C.albican
ZnO	12±0.12	16±0.12	11±0.20	9±0.20	13±0.20
6%N-ZnO	14 ±0.30	14 ±0.20	12±0.20	16±0.40	17±0.20
4%S-ZnO	12±0.12	17±0.20	13±0.30	16±0.20	12±0.30
S4-N6-ZnO	19±0.20	16.±0.31	14±0.40	18±0.20	18±0.2
Positive control(Genta and CLO)	29±0.30	30±0.40	26±0.20	27±0.30	21±0.20
Negative control(DMSO)	-	-	-	-	-

4.7 Antioxidant activity analysis

The radical scavenging properties of the un doped ZnO NPs, 6%Ndoped, 4%S doped and S4-N6-ZnO NPs evaluated through the DPPH method showed an increased RSA with an increase in the NPs' concentration. The NPs' half-maximal inhibitory concentration (IC50) were found to be 1 60.73, 50.20, 27.10, and 78.40 respectively (**Table 2**). It was also noted that the ZnO NPs and 6%N doped offer high antioxidant activity while 4%S doped and co doped have equal inhibition at 50 μg·mL−1[55]. This result indicates that the prepared S-N- co doped ZnO NPs can inhibit oxidation due to the transfer of electron density located at the oxygen atom to the nitrogen atom in the DPPH free radical, which contains an odd electron by n→π_ transition [59].

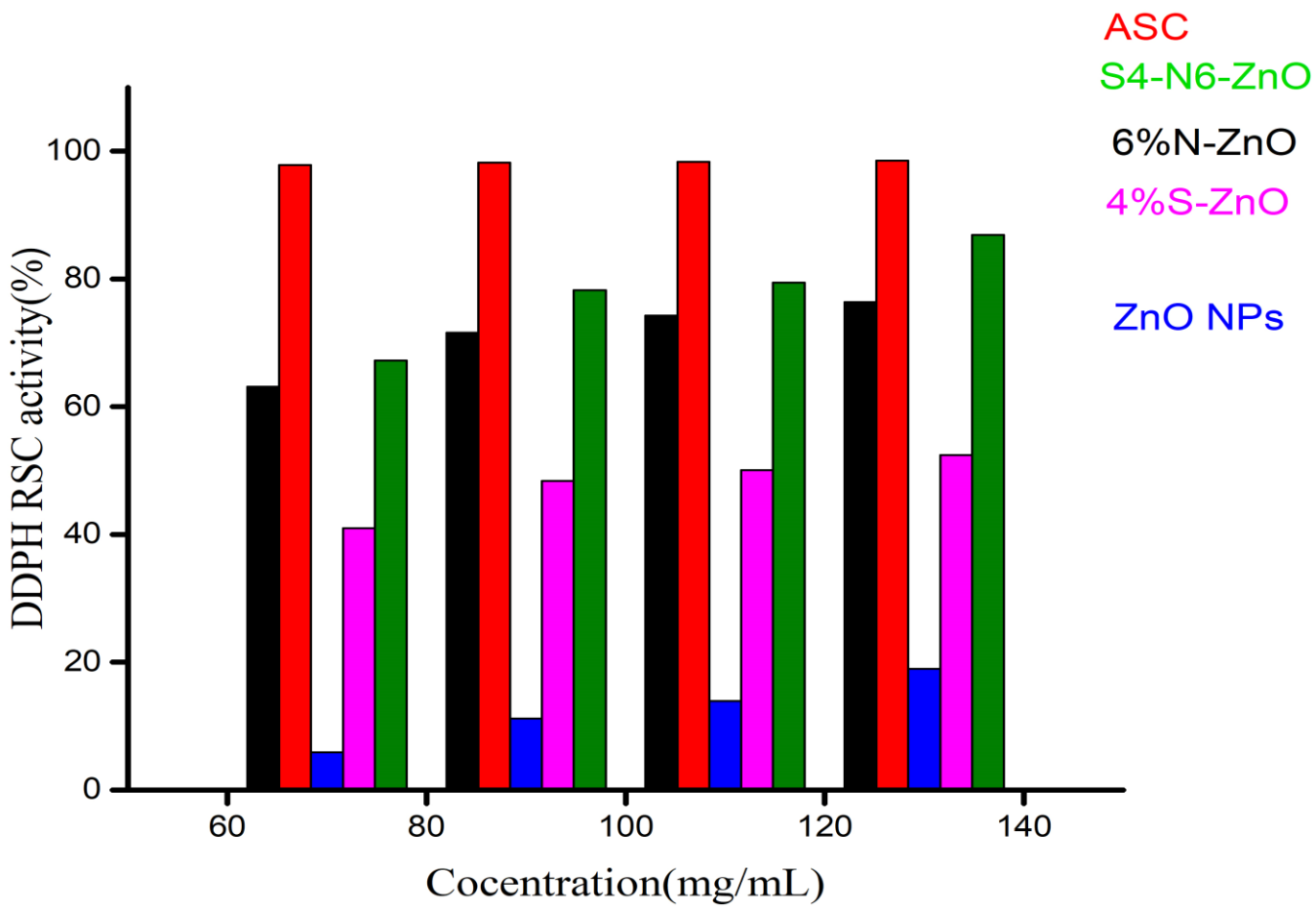

Figure 7. DDPH scavenging activity of ZnO-NPs, 6%N-ZnO, 4%S-ZnO and S4-N6-ZnO

Table3. DDPH radical scavenging assay

	Concentration(mg/mL)	%RSC of DDPH	IC50 (mg/mL)
ZnO-NPs	70	40.98380181	
	90	48.40400191	
	110	50.04764173	
	130	52.45354931	
			67.73840609

6%N-ZnO	70	68.16341115	
	90	71.59361601	
	110	74.24964269	
	130	76.36969986	
			50.19248396
4%S-ZnO	70	55.22868032	
	90	71.2720343	
	110	72.43925679	
	130	78.6922344	
			27.10025434
S4-N6-ZnO	70	65.895664602	
	90	71.20771796	
	110	81.89947594	
	130	88.94949976	
			78.40025434
Ascorbic acid	70	97.6680324	
	90	98.70152454	
	110	98.8325393	
	130	98.9231062	
			43.75954198

5. Conclusion

In the present work, the effect of sulfur and nitrogen doping and co-doping synthesized ZnO nanoparticles on the optical energy bandgap, antimicrobial and antioxidant activity of ZnO-NPs, grown by the sol−gel method, was studied and discussed. The XRD results showed some additional peak patterns with S-N-co-doped was observed which resulted from residual or incomplete converson of complexe compound S and N of synthesized nanoparticles even though a hexagonal structures of ZnO is not changed. From the XRD results, it was observed that there was slightly change in diffraction angle both towards the lower and higher angle in 6%N-ZnO, as a result of ionic radius and bond length difference respectively as it was reported in other literatures. Crysal size of synthesized NPs has been calculated using FWHM , and the size of N-S-dual doped ZnO NPs has smallest compare to the single doped and pure ZnO NPs .The UV absorption spectra showed redshifts from 370 toward 377 nm and 378 nm due to the nitrogen and

sulfur doping respectively while 370 towards 379 nm due to S-N-co doping. Generally, the bandgap energy was decreased from 2.97 to 2.78. eV with nitrogen doping and decreased from 2.97 to 2.69 eV with sulphur doping and finally decreased from 2.97 to 2.63 ev for S-N-co doping. Generally ,functionality modification of ZnO nanoparticles is achieved by this research result of the bandgap energy narrowed, increments of surface to volume ratio which improve the application towards antimicrobial and antioxidant activity of ZnO-NPs.

6. Recommendation

In this research, the issue related to photoctallyitic degration of pollutant from waste water has not bee done and it is better for reseachers to focus on this .Additionally regarding characterization ,it will be done on EDAX and TEM.

REFERENCE

[1]. Whang Thou-Jen,; Mu-Tao, H. ; Huang-Han, C. *Appl. Surf. Sci.* **2012**, 258, 2796

[2]. Rastogi, A.; Zivcak, M.; Sytar, O.; Kalaji, H. M.; He, X.; Mbarki,S.; Brestic, M. Impact of Metal and Metal Oxide Nanoparticles on Plant: A Critical Review. *Front. Chem.* **2017**, 5,

[3]. Espitia, P.J.P.; Otoni, C.G.; Soares, N.F.F. Chapter 34—Zinc Oxide Nanoparticles for Food Packaging Applications. In Antimicrobial Food Packaging; Barros-Velázquez, J., Ed.; Academic Press: San Diego, CA, USA, **2016**; pp. 425–431.

[4]. Laurenti, M.; Cauda, V. ZnO Nanostructures for Tissue Engineering Applications. Nanomaterials **2017**, 7, 374.

[5]. Park, J.K.; Kim, Y.-J.; Yeom, J.; Jeon, J.H.; Yi, G.-C.; Je, J.H.; Hahn, S.K. The Topographic E_ect of Zinc Oxide Nano flowers on Osteoblast Growth and Osseo integration. Adv. Mater. **2010**, 22, 4857–4861

[6]. Ciofani, G.; Genchi, G.G.; Mattoli, V. ZnO nanowire arrays as substrates for cell proliferation and dierentiation. Mater. Sci. Eng. C **2012**, 32, 341–347.

[7]. Lee, J.; Kang, B.S.; Hicks, B.; Chancellor, T.F.; Chu, B.H.; Wang, H.-T.; Keselowsky, B.G.; Ren, F.; Lele, T.P. The control of cell adhesion and viability by zinc oxide nanorods. Biomaterials **2008**, 29, 3743–3749

[8]. Si X, Liu Y, Wu X, et al. The interaction between oxygen vacancies and doping atoms in ZnO. Materials & Design, **2015**, 87: 969–973

[9]. K. W. Aga, M. T. Efa, and T. T. Beyene, "Effects of Sulfur Doping and Temperature on the Energy Bandgap of ZnO Nanoparticles and Their Antibacterial Activities," 2022, doi: 10.1021/acsomega.2c00647.

[10]. Kyung, H.; Lee J.; Choi, W. *Environ. Sci. Technol*. **2005**, 39, 2376.

[11]. Hasnidawani, J. N.; Azlina, H. N.; Norita, H.; Bonnia, N. N.;Ratim, S. Synthesis of ZnO Nanostructures Using Sol-Gel Method. Procedia Chem**. 2016**, 19, 211−216

[12]. Laurenti M, Lamberti A, Genchi GG, Roppolo I, Canavese G, Vitale-Brovarone C, Ciofani G, Cauda V. Graphene Oxide Finely Tunes the Bioactivity and Drug Delivery of Mesoporous ZnO Scaffolds. ACS Appl Mater Interfaces. **2019**; 11:449-456. DOI: 10.1021/acsami.8b20728

[13]. Lee, N.-Y.; Ko,W.-C.; Hsueh, P.-R. Nanoparticles in the Treatment of Infections Caused by Multi-drug Resistant Organisms. Front. Pharmacol. **2019**, 10, 1153.

[14]. Shargh, V.H.; Honder marck, H.; Liang, M. Antibody -targeted biodegradable nanoparticles for cancer therapy. Nanomedicine **2015**, 11, 63–79

[15]. Malik, R.; Tomer, V.K.; Mishra, Y.K.; Lin, L. Functional gas sensing nanomaterials: A panoramic view. Appl. Phys. Rev. **2020**, 7, 021301

[16]. Stassi, S.; Cauda, V.; Ottone, C.; Chiodoni, A.; Pirri, C.F.; Canavese, G. Flexible piezoelectric energy nano generator based on ZnO nanotubes hosted in a polycarbonate membrane. Nano Energy **2015**, 13, 474–48

[17]. Dumontel, B.; Canta, M.; Engelke, H.; Chiodoni, A.; Racca, L.; Ancona, A.; Limongi, T.; Canavese, G.; Cauda, V. Enhanced biostability and cellular uptake of zinc oxide nanocrystals shielded with a phospholipid bilayer. J. Mater. Chem. B **2017**, 5, 8799–8813.

[18]. Fu D, Han G, Chang Y, et al. The synthesis and properties of ZnO–graphene nano hybrid for photodegradation of organic pollutant in water. Materials Chemistry and Physics, **2012**, 132

[19]. (2–3): 673–681

[20]. Lee, H.-J.; Jeong, S.-Y.; Cho, C.R.; Park, C.H. Study of diluted magnetic semiconductor: Co-doped ZnO. Appl. Phys. Lett. **2002**, 81, 4020–4022.

[21]. Laurenti, M.; Garino, N.; Canavese, G.; Hernandéz, S.; Cauda, V. Piezo- and Photocatalytic Activity of Ferroelectric ZnO:Sb Thin Films for the E_cient Degradation of Rhodamine-_ dye Pollutant. ACS Appl. Mater. Interfaces **2020**, 12, 25798–25808.

[22]. Laurenti, M.; Castellino, M.; Perrone, D.; Asvarov, A.; Canavese, G.; Chiolerio, A. Lead-free piezoelectrics: V3+ to V5+ ion conversion promoting the performances of V-doped Zinc Oxide. Sci. Rep. **2017**, 7, 41957.

[23]. Aiswarya, S., et al.: Strategy of metal iron doping and green-mediated ZnO nanoparticles: dissolubility, antibacterial and cytotoxic traits. Toxicol. Res. 6(6), 854–865 (**2017**). https://doi.org/10.1039/c7tx00093f

[24]. Pradeev raj, K., et al.: Influence of Mg doping on ZnO nanoparticles for enhanced photocatalytic evaluation and antibacterial analysis. Nanoscale Res. Lett. 13, 229 (**2018**). https://doi.org/10.1186/s11671-018-2643-x

[25]. Guo, B.L., et al.: The antibacterial activity of Ta-doped ZnO nanoparticles. Nanoscale Res. Lett. 10, 336 (**2015**). https://doi.org/10.1186/ s11671-015-1047-4

[26]. Carofiglio, M., et al.: Doped zinc oxide nanoparticles: synthesis, characterization and potential use in nanomedicine. Appl. Sci. 10,519(**2020**). https://doi.org/10.3390/app1015519413

[27]. Hussain, A., et al.: Biogenesis of ZnO nanoparticles using *Pandanus odorifer* leaf extract: anticancer and antimicrobial activities. RSC Adv. 9, 15357–15369 (**2019**). https://doi.org/10.1039/c9ra01659g

[28]. Chauhan, A., et al.: Photocatalytic dye degradation and antimicrobial activities of Pure and Ag-doped ZnO using *Cannabis sativa* leaf extract. Sci. Rep. 10, 7881 (**2020**). https://doi.org/10.1038/s41598-020-64419-0

[29]. Samadi, M.; Zirak, M.; Naseri, A.; Khorashadizade, E.; Moshfegh, A.Z. Recent progress on doped ZnO nanostructures for visible-light photocatalysis. Thin Solid Film. **2016**, 605, 2–19.

[30]. Cerrato, E.; Gionco, C.; Berruti, I.; Sordello, F.; Calza, P.; Paganini,M.C. Rare earth ions doped ZnO: Synthesis, characterization and preliminary photoactivity assessment. J. Solid State Chem. **2018**, 264, 42–47.

[31]. Kumar, V.; Ntwaea borwa, O.M.; Soga, T.; Dutta, V.; Swart, H.C. Rare Earth Doped Zinc Oxide Nanophosphor Powder: A Future Material for Solid State Lighting and Solar Cells. ACS Photonics **2017**, 4, 2613–2637

[32]. Patil A B, Patil K R, Pardeshi S K. Ecofriendly synthesis and solar photocatalytic activity of S-doped ZnO. Journal of Hazardous Materials, **2010**, 183(1–3): 315–323

[33]. Zhou P, Yu X, Yang L, et al. Simple air oxidation synthesis and optical properties of S-doped ZnO microspheres. Materials Letters, **2007**, 61(18): 3870–3872

[34]. Darzi S J, Mahjoub A, Bayat A. Sulfur modified ZnO nanorod as a high performance photo catalyst for degradation of Congoredazo dye. International Journal of Nano Dimension, **2015**, 6(4): 425–431

[35]. Long S, Li Y, Yao B, et al. Effect of doping behaviors of Ag and S on the formation of p-type Ag–S co-doped ZnO film by a modified hydrothermal method. Thin Solid Films, **2016**, 600: 13–18

[36]. Cruz-Vázquez C, Rocha-Alonzo F, Burruel-Ibarra S E, et al. Fabrication and characterization of sulfur doped zinc oxide thin films. Superficies y Vacío, **2001**, 13: 89–91

[37]. Wang X H, Liu S, Chang P, et al. Influence of S incorporation on the luminescence property of ZnO nanowires by electrochemical deposition. Physics Letters A, **2008**, 372(16): 2900–2903

[38]. Shen G, Cho J H, Yoo J K, et al. Synthesis and optical properties of S-doped ZnO nanostructures: nanonails and nanowires. The Journal of Physical Chemistry B, **2005**, 109(12): 5491–5496

[39]. Wang X H, Liu S, Chang P, et al. Synthesis of sulfur-doped ZnO nanowires by electrochemical deposition. Materials Science in Semiconductor Processing, **2007**, 10(6): 241–245

[40]. Long S, Li Y, Yao B, et al. Effect of doping behaviors of Ag and S on the formation of p-type Ag–S co-doped ZnO film by a modified hydrothermal method. Thin Solid Films, **2016**, 600: 13–18

[41]. Yan Y, Al-Jassim M M, Wei S H. Doping of ZnO by group-IB elements. Applied Physics Letters, **2006**, 89(18): 181912

[42]. Janotti, A.;van de Walle, C.G. Fundamentals of zinc oxide as a semiconductor. *Rep. Prog. Phys.* **2009**, *72*, 126501.

[43]. Lim, J.-H.; Kang, C.-K.; Kim, K.-K.; Park, I.-K.; Hwang, D.-K.; Park, S.-J. UV-vis Electro luminescence Emission from Zn Light- Emitting Diodes Grown by High Temperature Radiofrequency Sputtering. *Adv. Mater.* **2006**, *18*, 2720–2724.

[44]. Sun, J.C.; Zhao, J.Z.; Liang, H.W.; Bian, J.M.; Hu, L.Z.; Zhang, H.Q.; Liang, X.P.; Liu, W.F.; Du, G.T. Realization of ultraviolet electroluminescence from ZnO homo junction with n-ZnO⁄p-ZnO: As⁄GaAs structure. *Appl. Phys. Lett.* **2007**, *90*, 121128.

[45]. Kong, J.; Chu, S.; Olmedo, M.; Li, L.; Yang, Z.; Liu, J. Dominant ultraviolet light emissions in packed ZnO columnar homo junction diodes. *Appl. Phys. Lett.* **2008**, *93*, 132113.

[46]. Li, Z.; Suyuan, S.; Xiao, X.; Bin, Z.; Alan, M. *Catal. Commun.* **2011**, 12, 890

[47]. Yamamoto, T.; Katayama-Yoshida, H. Physics and control of valence states in ZnO by codoping method. Phys. B Condens. Matter **2001**, 302–303, 155–162.

[48]. Thang, H.V.; Pham, T.L.M.; Pacchioni, G. DFT study of electronic properties of N-doped ZnO and ZnO/Cu bilayer films. Surf. Sci. **2022**, 716, 121978.

[49]. A. B. V. K. Kumar, S. Billa, and G. Shankar, "C, N dual-doped ZnO nanofoams : a potential antimicrobial agent, an efficient visible light photocatalyst and SXAS studies research papers," pp. 90–99, 2020, doi: 10.1107/S160057751901364X.

[50]. R. C. De Souza, L. U. Haberbeck, H. G. Riella, D. H. B. Ribeiro, and B. A. M. Carciofi, "ANTIBACTERIAL ACTIVITY OF ZINC OXIDE NANOPARTICLES SYNTHESIZED BY SOLOCHEMICAL PROCESS," vol. 36, no. 02, pp. 885–893, 2019.

[51]. X. Biotech, J. Jose, and S. Asokan, "Characterization and evaluation of the antibacterial potential of ZnO nanoparticle synthesized by Vigna Mungo and Rhizobacteria Characterization ad evaluation of antibacterial potential of ZnO nanoparticle synthesized by

Vigna Mungo and Rhizobacteria,” no. June, 2021.

[52]. A. S. Al-gurabi, S. Al-ani, and E. A. Al-ajaj, “Preparation and characterization of ZnO nano-particles ةيوناننالا كنزلا ذيسكوا تابيبح صاوخ ةسارد ريضحت,” pp. 24–34.

[53]. S. Singh, T. Mahajan, K. Kaur, and F. Sahib, “Synthesis , Characterization and Effect of Increasing Nitrogen Concentration on the Growth of ZnO Nanoparticles,” vol. 6, no. 3, pp. 1–11, 2018, doi: 10.4172/2321-6212.1000225.

[54]. G. Faye, “Euphorbia abyssinica bark extract,” no. June 2021, pp. 25–32, 2022, doi: 10.1049/nbt2.12072.

[55]. [G. Processing, B. L. Manjula, M. Mahadevamurthy, and A. Rahdar, “Antioxidant and photocatalytic properties of zinc oxide nanoparticles phyto - fabricated using the aqueous leaf extract of Sida acuta,” no. September, 2022, doi: 10.1515/gps-2022-0075.

[56]. S. Shahid, U. Fatima, R. Sajjad, and S. A. Khan, “BIOINSPIRED NANOTHERANOSTIC AGENT : ZINC OXIDE ; GREEN SYNTHESIS AND BIOMEDICAL POTENTIAL,” vol. 14, no. 4, pp. 1023–1031, 2019.

[57]. V. Kumari, A. Mittal, J. Jindal, S. Yadav, and N. Kumar, “S- , N- and C-doped ZnO as semiconductor photocatalysts : A review,” vol. 13, no. 1, pp. 1–22, 2019.

[58]. N. Sivakumar and R. Saranya, “Synthesis , Characterization and Evaluation of Zno and Copper – Nitrogen Co Doped Zinc Oxide (Cu-N-Zno) Nanoparticles for Its Biological Applications,” no. 1, pp. 16–20, 2017.

[59]. F. Rahman, A. M. Patwary, A. B. Siddique, S. Bashar, A. Haque, and B. Akter, “Green synthesis of zinc oxide nanoparticles using Cocos nucifera leaf extract : characterization , antimicrobial , antioxidant and photocatalytic activity,” 2022.

Appendinces

Appendix 1: A. Ultraviolet-visible absorbance spectra of bare, doped and co doped quantities of nitrogen and sulphur zincoxides**.**

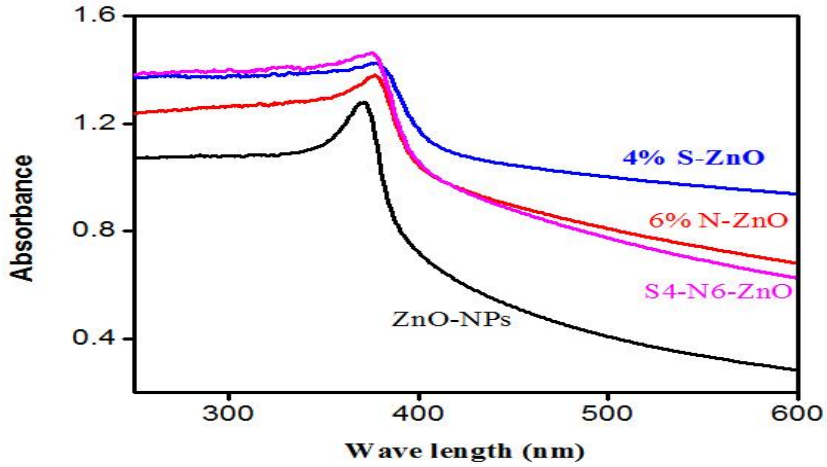

APPendix2: Energy Bandgaps of bare doped co-doped quantities of nitrogen and Sulphur. (a) Pure ZnO-NPs (b) 6%N-ZnO (c) 4%S-ZnO and (d) S4-N6-ZnO

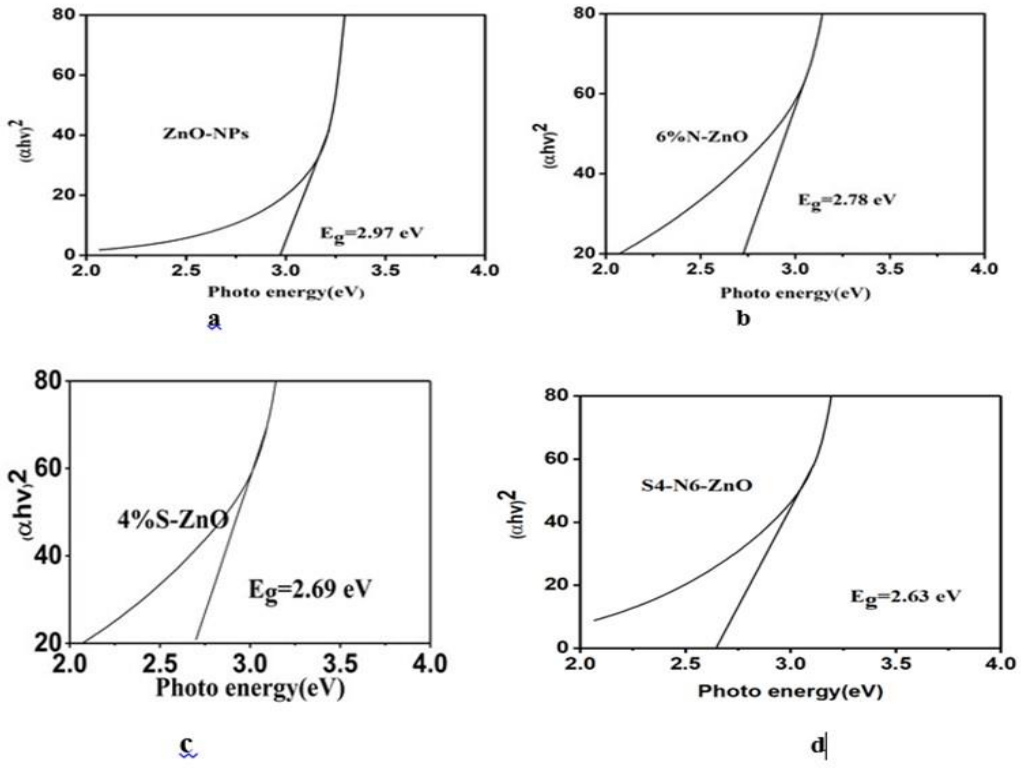

Appendix3: XRD pattern of pure ZnO-NPs, 6%N-ZnO, 4%S-ZnO and S4-N6-ZnO.

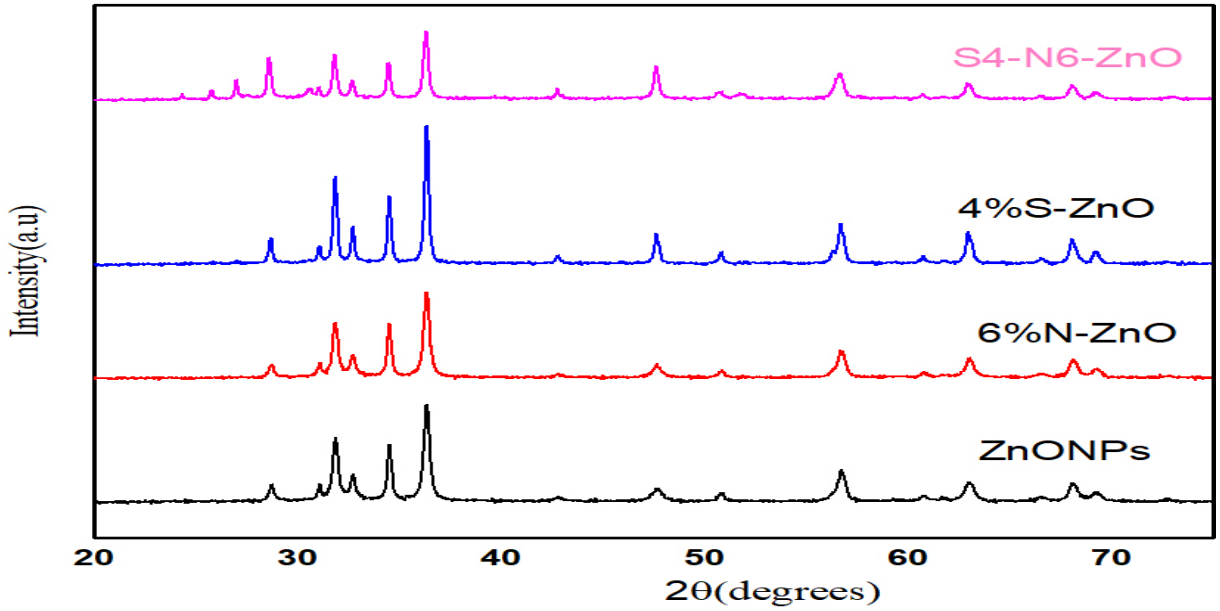

Appendix 4: Diagrams showing of zone of inhibition the pure and doped ZnO-NPs against some selected microorganisms

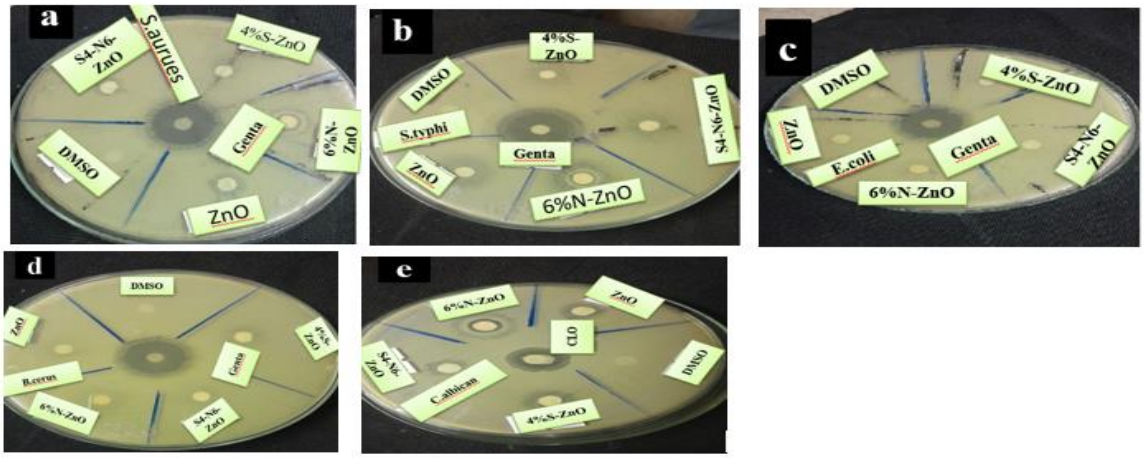

Appendix 5: DDPH radical scavenging assay

	Concentration(mg/mL)	%RSC of DDPH	IC50 (mg/mL)
ZnO-NPs	70	40.98380181	
	90	48.40400191	
	110	50.04764173	
	130	52.45354931	
			67.73840609
6%N-ZnO	70	68.16341115	
	90	71.59361601	
	110	74.24964269	
	130	76.36969986	
			50.19248396
4%S-ZnO	70	55.22868032	
	90	71.2720343	
	110	72.43925679	
	130	78.6922344	
			27.10025434
S4-N6-ZnO	70	65.895664602	
	90	71.20771796	
	110	81.89947594	
	130	88.94949976	
			78.40025434
Ascorbic acid	70	97.6680324	
	90	98.70152454	
	110	98.8325393	
	130	98.9231062	
			43.75954198